

# Phase II Study of a Radiotherapy Total Dose Increase in Hypoxic Lesions Identified by $^{18}\text{F}$ -Misonidazole PET/CT in Patients with Non–Small Cell Lung Carcinoma (RTEP5 Study)

Pierre Vera<sup>1</sup>, Sébastien Thureau<sup>2</sup>, Philippe Chaumet-Riffaud<sup>3</sup>, Romain Modzelewski<sup>1</sup>, Pierre Bohn<sup>1</sup>, Maximilien Vermandel<sup>4</sup>, Sébastien Hapdey<sup>1</sup>, Amandine Pallardy<sup>5</sup>, Marc-André Mahé<sup>6</sup>, Marie Lacombe<sup>7</sup>, Pierre Boisselier<sup>8</sup>, Sophie Guillemard<sup>9</sup>, Pierre Olivier<sup>10</sup>, Veronique Beckendorf<sup>11</sup>, Naji Salem<sup>12</sup>, Nathalie Charrier<sup>13</sup>, Enrique Chajon<sup>14</sup>, Anne Devillers<sup>15</sup>, Nicolas Aide<sup>16</sup>, Serge Danhier<sup>17</sup>, Fabrice Denis<sup>18</sup>, Jean-Pierre Muratet<sup>19</sup>, Etienne Martin<sup>20</sup>, Alina Berriolo Riedinger<sup>21</sup>, Hélène Kolesnikov-Gauthier<sup>22</sup>, Eric Dansin<sup>23</sup>, Carole Massabeau<sup>24</sup>, Frédéric Courbon<sup>25</sup>, Marie-Pierre Farcy Jacquet<sup>26</sup>, Pierre-Olivier Kotzki<sup>9,27</sup>, Claire Houzard<sup>28</sup>, Françoise Mornex<sup>29</sup>, Laurent Vervueren<sup>30</sup>, Amaury Paumier<sup>31</sup>, Philippe Fernandez<sup>32</sup>, Mathieu Salaun<sup>33</sup>, and Bernard Dubray<sup>2</sup>

<sup>1</sup>Department of Nuclear Medicine, Henri Becquerel Cancer Center and Rouen University Hospital & QuantIF–LITIS, University of Rouen, Rouen, France; <sup>2</sup>Department of Radiation Oncology and Medical Physics, Henri Becquerel Cancer Center and Rouen University Hospital & QuantIF–LITIS, Rouen, France; <sup>3</sup>Department of Nuclear Medicine, Hôpitaux universitaires Paris Sud Bicêtre AP-HP and University Paris Sud, Paris, France; <sup>4</sup>University Lille, Inserm, CHU Lille, U1189–ONCO-THAI–Image Assisted Laser Therapy for Oncology, Lille, France; <sup>5</sup>Department of Nuclear Medicine, Nantes University Hospital, Nantes, France; <sup>6</sup>Department of Radiation Oncology, Institut de Cancérologie de l'Ouest (ICO)–René Gauducheau, Nantes, France; <sup>7</sup>Department of Nuclear Medicine, Institut de Cancérologie de l'Ouest (ICO), Nantes, France; <sup>8</sup>Department of Radiation Oncology, Institut régional du Cancer Montpellier (ICM), Montpellier, France; <sup>9</sup>Department of Nuclear Medicine, Institut régional du Cancer Montpellier (ICM), Montpellier, France; <sup>10</sup>Department of Nuclear Medicine, Brabois University Hospital, Nancy, France; <sup>11</sup>Department of Radiation Oncology, Institut de Cancérologie de Lorraine, Nancy, France; <sup>12</sup>Department of Radiation Oncology, Institut Paoli Calmette, Marseille, France; <sup>13</sup>Department of Nuclear Medicine, Institut Paoli Calmette, Marseille, France; <sup>14</sup>Department of Radiation Oncology, Centre regional de lutte contre le cancer de Bretagne Eugène Marquis, Rennes, France; <sup>15</sup>Department of Nuclear Medicine, Centre regional de lutte contre le cancer de Bretagne Eugène Marquis, Rennes, France; <sup>16</sup>Nicolas Aide, Nuclear Medicine and TEP Centre, Caen University Hospital and Inserm U1086 ANTICIPE, Caen, France; <sup>17</sup>Department of Radiation Oncology, François Baclesse Cancer Center, Caen, France; <sup>18</sup>Department of Radiation Oncology, Institut Inter-Régional de Cancérologie (ILC), Centre Jean Bernard/Clinique Victor Hugo, Le Mans, France; <sup>19</sup>Department of Nuclear Medicine, Institut Inter-Régional de Cancérologie (ILC), Centre Jean Bernard/Clinique Victor Hugo, Le Mans, France; <sup>20</sup>Radiation Oncology, Centre Georges-François Leclerc, Dijon, France; <sup>21</sup>Department of Nuclear Medicine, Centre Georges François Leclerc, Dijon, France; <sup>22</sup>Department of Nuclear Medicine, Oscar Lambret Center, Lille cedex, France; <sup>23</sup>Department of Radiation Oncology, Oscar Lambret Center, Lille cedex, France; <sup>24</sup>Département de Radiothérapie, Institut Universitaire du Cancer, Toulouse cedex 9, France; <sup>25</sup>Department of Nuclear Medicine, Institut Claudius Regaud, IUCT, Toulouse cedex 9, France; <sup>26</sup>Department of Radiation Oncology, CHU de Nîmes, Institut de Cancérologie du Gard, Rue Henri Pujol, Nîmes, France; <sup>27</sup>Department of Nuclear Medicine, CHU de Nîmes, Institut de Cancérologie du Gard, Nîmes, France; <sup>28</sup>Department of Nuclear Medicine, Hospices Civils de Lyon, Lyon, France; <sup>29</sup>Department of Radiation Oncology, Hospices Civils de Lyon, Lyon, France; <sup>30</sup>Department of Nuclear Medicine, CHU Angers, France; <sup>31</sup>Department of Radiation Oncology, Institut de Cancérologie de l'Ouest, site Paul Papin, France; <sup>32</sup>Department of Nuclear Medicine, Hôpital Pellegrin, CHU de Bordeaux, France; and <sup>33</sup>Normandy University, UNIROUEN, QuantIF–LITIS EA 4108, Rouen University Hospital, Department of Pulmonology–Thoracic Oncology–Respiratory Intensive Care, Rouen, France

See an invited perspective on this article on page 1043.

This multicenter phase II study investigated a selective radiotherapy dose increase to tumor areas with significant  $^{18}\text{F}$ -misonidazole ( $^{18}\text{F}$ -FMISO) uptake in patients with non–small cell lung carcinoma (NSCLC). **Methods:** Eligible patients had locally advanced NSCLC

and no contraindication to concomitant chemoradiotherapy. The  $^{18}\text{F}$ -FMISO uptake on PET/CT was assessed by trained experts. If there was no uptake, 66 Gy were delivered. In  $^{18}\text{F}$ -FMISO–positive patients, the contours of the hypoxic area were transferred to the radiation oncologist. It was necessary for the radiotherapy dose to be as high as possible while fulfilling dose-limiting constraints for the spinal cord and lungs. The primary endpoint was tumor response (complete response plus partial response) at 3 mo. The secondary endpoints were toxicity, disease-free survival (DFS), and overall survival at 1 y. The target sample size was set to demonstrate a response rate of 40% or more (bilateral  $\alpha = 0.05$ , power  $1-\beta = 0.95$ ). **Results:** Seventy-nine patients were preinformed, 54 were included, and 34 were  $^{18}\text{F}$ -FMISO–positive, 24 of whom received escalated doses of up to 86 Gy. The response rate at 3 mo was 31 of 54 (57%; 95% confidence interval [CI], 43%–71%) using RECIST 1.1 (17/34 responders in the  $^{18}\text{F}$ -FMISO–positive group).

Received Dec. 8, 2016; revision accepted Feb. 7, 2017.

For correspondence contact: Pierre Vera, Department of Nuclear Medicine, Henri Becquerel Cancer Center and Rouen University Hospital & QuantIF–LITIS [EA (Equipe d'Accueil) 4108–FR CNRS 3638], Faculty of Medicine, University of Rouen, Rouen, France.

E-mail: pierre.vera@chb.unicancer.fr

Published online Mar. 2, 2017.

COPYRIGHT © 2017 by the Society of Nuclear Medicine and Molecular Imaging.

DFS and overall survival at 1 y were 0.86 (95% CI, 0.77–0.96) and 0.63 (95% CI, 0.49–0.74), respectively. DFS was longer in the  $^{18}\text{F}$ -FMISO–negative patients ( $P = 0.004$ ). The radiotherapy dose was not associated with DFS when adjusting for the  $^{18}\text{F}$ -FMISO status. One toxic death (66 Gy) and 1 case of grade 4 pneumonitis (>66 Gy) were reported. **Conclusion:** Our approach results in a response rate of 40% or more, with acceptable toxicity.  $^{18}\text{F}$ -FMISO uptake in NSCLC patients is strongly associated with poor prognosis features that could not be reversed by radiotherapy doses up to 86 Gy.

**Key Words:** positron emission tomography; fluoro-deoxy-D-glucose; f-misonidasole; hypoxia; lung cancer; radiotherapy dose

**J Nucl Med 2017; 58:1045–1053**

DOI: 10.2967/jnumed.116.188367

**R**adiotherapy is a major component in the treatment of non-resectable locally advanced non–small cell lung cancer (NSCLC) (1). Although concomitant radiochemotherapy (CCRT) is the current standard for curative-intent treatment, the tumor control rate and survival probabilities remain disappointing. Improvements in radiotherapy techniques should yield better intrathoracic control; a reduction in secondary distant dissemination; less normal-tissue damage; and as a consequence, reduced mortality caused by cancer, toxicity, or worsening of preexisting comorbidities. The identification of the adequate target volumes and the delivery of sufficiently high total doses are closely linked. Phase II studies have shown that higher doses could only be delivered to smaller target volumes (2,3). The RTOG 0617 randomized trial reported lower survival probabilities in the patients having received more than 60 Gy, possibly because the target volumes were too large (4). Therefore, it is tempting to reduce the target volumes and escalate the radiotherapy dose only to the most aggressive parts of the tumor. For example, the dose could be selectively increased in the tumor areas with the highest  $^{18}\text{F}$ -FDG uptake (5,6). Because oxygen is the most powerful radiosensitizer (7), we hypothesized that the hypoxic areas in the tumor would be relevant targets for selective dose escalation.

In a phase II study, we used  $^{18}\text{F}$ -misonidazole ( $^{18}\text{F}$ -FMISO), a PET/CT tracer for hypoxic cells, to identify and delineate hypoxic areas as biologic target volumes (BTVs) for escalated total dose radiotherapy associated with concomitant chemotherapy. A rigorous quality assurance protocol was set to ensure that all PET/CT images were acquired under reproducible conditions. The presence of  $^{18}\text{F}$ -FMISO uptake was assessed by consensus by trained experts (8). The BTVs were centrally delineated. The primary endpoint was the tumor response at 3 mo after CCRT. The secondary endpoints were acute and late toxicity, as well as disease-free survival (DFS) and overall survival (OS) at 1 y.

## MATERIALS AND METHODS

### Study Design and Patients

The design of the study is described in Figure 1. Between June 6, 2012, and March 19, 2015, the patients with NSCLC referred to the participating centers for CCRT were prospectively preincluded. Fifteen academic centers included patients into the study.

The main inclusion criteria were age older than 18 y; histologic proof of NSCLC with a measurable tumor (RECIST1.1); World Health Organization performance status of 1 or less; eligibility for curative-intent CCRT (no pleural, pulmonary, or extrathoracic metastases and no comorbidity contraindicating CCRT); adequate lung function (forced expiratory volume  $\geq 40\%$  and diffusing capacity of the lung

(divided by the alveolar volume  $\geq 50\%$  of the predicted values;  $\text{PaO}_2 \geq 60$  mm Hg); a neutrophil count of more than  $1.5 \times 10^9$  cells/L, platelet count more than  $100 \times 10^9$ /L, and hemoglobin more than 10 g/dL; and an estimated creatinine clearance of more than 60 mL/min. All patients had to receive cisplatin-based chemotherapy as the induction treatment and concomitantly with radiotherapy. Inclusion was confirmed after completion of a radiotherapy plan confirming that the dose objective (a minimum dose of 60 Gy in 99% of the planning target volume) and the constraints (lungs, spinal cord) could be met.

The noninclusion criteria were histology other than primary NSCLC; a nonevaluable lesion (complete remission after induction chemotherapy); no uptake or metastases on the first acquisition of  $^{18}\text{F}$ -FDG PET/CT ( $^{18}\text{F}$ -FDG<sub>1</sub> PET/CT) performed after the induction chemotherapy and before CCRT; contraindication of curative-intent radiotherapy (tumor extension, World Health Organization performance status  $\geq 2$ , coexistent disease); synchronous cancer or previous malignancy within 5 y before inclusion; patient already participating in another clinical trial; confirmed or suspected pregnancy and lactating females; renal insufficiency contraindicating cisplatin treatment; patients under legal protection; inability to comply with the follow-up procedures for geographic, social, or psychologic reasons; uncontrolled diabetes mellitus (blood glucose  $\geq 10$  mmol/L); and patients unable to give informed consent.

The eligible patients had to have at least 1  $^{18}\text{F}$ -FDG–avid lesion at  $^{18}\text{F}$ -FDG<sub>1</sub> PET/CT. These patients were then considered to have hypoxic lesions if significant  $^{18}\text{F}$ -FMISO uptake was observed in the  $^{18}\text{F}$ -FDG–avid lesions on a subsequent first  $^{18}\text{F}$ -FMISO performed before CCRT ( $^{18}\text{F}$ -FMISO<sub>1</sub>) PET/CT scan within 8 d. The evaluable population was formed from all the eligible patients who completed the protocol (a complete mandatory dataset is included at the end of the study). The patients who eventually withdrew their consent to participate were not evaluated.

The protocol and the consent form were approved by the Comité de Protection des Personnes Nord-Ouest 1 (July 21, 2011). All patients gave their written, informed consent. The study was registered in the Clinical Trials Protocol Registration System (NCT01576796; RTEP5 study). The clinical, biologic, imaging, and toxicities data were monitored by a certified clinical research unit.

### PET Imaging

The PET/CT machines were Biograph Sensation 16 (Siemens), Gemini (Philips), or Discovery LS (GE Healthcare). For each patient, 2  $^{18}\text{F}$ -FDG PET/CT and 2  $^{18}\text{F}$ -FMISO PET/CT scans were acquired using the same machine and under the identical operational conditions. Quality control (QC) was centrally supervised to secure homogeneity in the image quality in all participating centers. The QC procedures and results are provided in the supplemental materials (available at <http://jnm.snmjournals.org>).

The  $^{18}\text{F}$ -FDG PET images were acquired in treatment position (arms over the head, free breathing), at least 15 d after the last administration of chemotherapy. No chemotherapy was allowed between the PET/CT and the start of radiotherapy. Six to 8 bed positions per patient were acquired from the head to the upper third of the thighs. The images were acquired at a minimum of  $60 \pm 10$  min after the  $^{18}\text{F}$ -FDG injection. The patients were required to fast overnight or for at least 6 h before the imaging to ensure that the serum glucose and endogenous serum insulin levels were low at the time of the  $^{18}\text{F}$ -FDG administration. The blood glucose levels were measured before each  $^{18}\text{F}$ -FDG PET acquisition. A total of 4.5 MBq/kg were administered intravenously after a rest period of at least 20 min. The first acquisition ( $^{18}\text{F}$ -FDG<sub>1</sub>) after the induction chemotherapy started at  $T_1 = 60 \pm 10$  min after injection. The second  $^{18}\text{F}$ -FDG PET ( $^{18}\text{F}$ -FDG<sub>2</sub>) was performed during the fifth week of radiotherapy at a total dose of 40–46 Gy as previously demonstrated (9). The acquisition procedure followed conditions identical to those for  $^{18}\text{F}$ -FDG<sub>1</sub>, specifically, with a  $T_2 = T_1 \pm 5$  min.

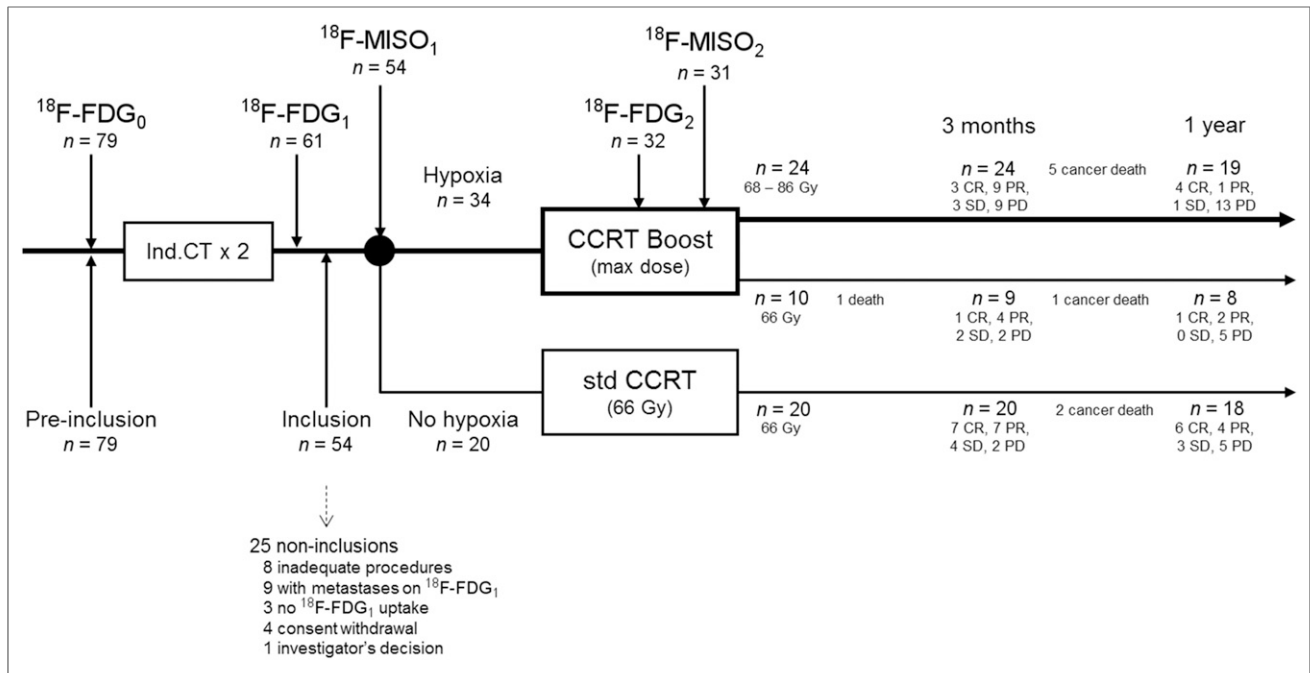


**FIGURE 1.** Study design/study flow. SD = stable disease; PD = progressive disease (RECIST 1.1).

The  $^{18}\text{F-FMISO}$  PET images were acquired under identical conditions. Two to 3 bed positions per patient were acquired for the thorax. The images were acquired at a minimum of  $240 \pm 20$  min after the  $^{18}\text{F-FMISO}$  injection. A total of 4.5 MBq/kg were administered intravenously after

**TABLE 1**  
Baseline Characteristics of 54 Included Patients

Characteristic	Hypoxia, trial arm			No hypoxia	
	Total (n = 34)	Boost (n = 24)	66 Gy (n = 10)	66 Gy (n = 20)	Total (n = 54)
<b>Sex (n)</b>					
Female	6	4	2	1	7
Male	28	20	8	19	47
Mean age $\pm$ SD (y)	59.5 $\pm$ 8.6	60.5 $\pm$ 8.4	57.2 $\pm$ 9.2	61.4 $\pm$ 5.7	60.3 $\pm$ 7.7
Mean height $\pm$ SD (cm)	169.7 $\pm$ 9.3	171.1 $\pm$ 10.1	166.6 $\pm$ 6.1	170.3 $\pm$ 8.1	170.0 $\pm$ 8.8
Mean weight $\pm$ SD (kg)	73.2 $\pm$ 14.6	71.5 $\pm$ 12.3	77.2 $\pm$ 19.2	76.5 $\pm$ 12.1	74.4 $\pm$ 13.7
<b>Histology (n)</b>					
SCC	17	14	3	9	26
ADC	11	6	5	10	21
Undifferentiated	6	4	2	1	7
<b>Tumor stage (n)</b>					
IB	1	1	—	1	2
IIA	—	—	—	1	1
IIB	2	1	1	0	2
IIIA	17	13	4	7	24
IIIB	13	8	5	11	24
IV	1	1	—	—	1
Mean radiotherapy dose $\pm$ SD (Gy)	73.9 $\pm$ 6.7	77.1 $\pm$ 5.2*	66 $\pm$ 0	66 $\pm$ 0.4	71 $\pm$ 6.5

\*Significantly different from 66-Gy group ( $P < 0.0001$ ).

SCC = squamous cell carcinoma; ADC = adenocarcinoma.

**TABLE 2**  
PET Data of 54 Included Patients

Characteristic	Hypoxia, trial arm			No hypoxia		P
	Total (n = 34)	Boost (n = 24)	66 Gy (n = 10)	66 Gy (n = 20)	Total (n = 54)	
<b><sup>18</sup>F-FDG SUV<sub>max</sub></b>						
PET1 (n = 54)	14.5 ± 9.3	13.8 ± 7.8	16.4 ± 12.4	8.4 ± 9.0	10.0 ± 0.7	0.021
PET2 (n = 32)	9.4 ± 6.1*	10 ± 7.1*	8.1 ± 4.0*	—	—	
Δ(%)	-32 ± 26	-27 ± 29	-44 ± 17	—	—	
<b><sup>18</sup>F-FDG<sub>BTV</sub> (BTV<sub>m</sub>) @ 40% SUV<sub>max</sub> (cc)</b>						
PET1 (n = 54)	55.4 ± 72.2	58.9 ± 84.8	46.8 ± 24.9	27.3 ± 23.9	45.0 ± 60.3	0.026
PET2 (n = 32)	36.1 ± 44.6*	39.9 ± 52.5	27.4 ± 17.6	—	—	
Δ(%)	-10 ± 226	-27 ± 271	-26 ± 41	—	—	
<b><sup>18</sup>F-FMISO SUV<sub>max</sub></b>						
PET1 (n = 54)	2.5 ± 0.7	2.4 ± 0.6	2.7 ± 0.9	1.4 ± 0.5	2.1 ± 0.8	<0.001
PET2 (n = 31)	1.9 ± 0.5*	1.8 ± 0.4*	2.2 ± 0.6	—	—	
Δ(%)	-17 ± 24	-21 ± 20	-8 ± 39	—	—	
<b><sup>18</sup>F-FMISO<sub>BTV</sub> (BTV<sub>h</sub>) @ 1.4 SUV (cc)</b>						
PET1 (n = 54)	33.5 ± 52.2	34.1 ± 58.1	31.9 ± 37.9	—	—	
PET2 (n = 31)	20.9 ± 34.6	18.9 ± 37.4	25.4 ± 28.9	—	—	
Δ(%)	-24 ± 75	-20 ± 84	-34 ± 44	—	—	

\*Significantly different from PET1 ( $P < 0.05$ ).

PET1 = PET after induction chemotherapy; PET2 = PET during radiotherapy.

Data are mean ± SD.  $P$  values are for comparisons between trial-arm ( $n = 34$ ) and no-hypoxia groups ( $n = 20$ ).

a rest period of at least 10 min. A first <sup>18</sup>F-FMISO PET (<sup>18</sup>F-FMISO<sub>1</sub>) was scheduled after induction chemotherapy, 48 h after the <sup>18</sup>F-FDG<sub>1</sub>. The second <sup>18</sup>F-FMISO PET (<sup>18</sup>F-FMISO<sub>2</sub>) was performed during the fifth week of radiotherapy, within 48 h after the <sup>18</sup>F-FDG<sub>2</sub>.

For all the <sup>18</sup>F-FDG and <sup>18</sup>F-FMISO acquisitions, the CT scan data were used for random coincidences, scatter and attenuation correction, and anatomic localization. The PET images (<sup>18</sup>F-FDG and <sup>18</sup>F-FMISO) were fused with the CT scan images. The <sup>18</sup>F-FMISO PET images were finally smoothed with a gaussian filter (full width at half maximum, 5 mm).

### PET Analysis

We previously showed (8) that the assessment of <sup>18</sup>F-FMISO/<sup>18</sup>F-FDG uptake (presence vs. absence) was reproducible in a multicenter setting. In this study, 3 independent experts (of 9) reviewed the <sup>18</sup>F-FMISO PET acquisitions and decided on the presence or absence of uptake within 48 h.

Because the interobserver agreement for the <sup>18</sup>F-FMISO volume measurements was low (8), all images were centrally delineated in a single center (Rouen) by a nuclear physician and a radiation oncologist, via a dedicated network (Imagys Interface [QI/QO/QA/QC] and Keosis workstation). (Keosis Imagys Interface [QI/QO/QA/QC] is 21-CFR part 11-compliant. The Keosis company is ISO 9001 and ISO 13485 medical device-compliant. Images were stored and archived on a dedicated IIA class server.) For each patient, the CT image of PET <sup>18</sup>F-FDG and <sup>18</sup>F-FMISO was first coregistered to the planning CT scan (version 1.4, Oncoplanet; DosiSoft) with registration based on the lesion. The volumes of interest for <sup>18</sup>F-FDG metabolic biological target volume (BTV<sub>m</sub>) were defined as the sum of the pixels above 40% of the SUV<sub>max</sub> inside the primary tumor or nodes (10). The volumes of <sup>18</sup>F-FMISO (biologic hypoxic target volume [BTV<sub>h</sub>]) were defined as

the sum of pixels with an SUV 1.4 or more as previously validated (8). The coregistered <sup>18</sup>F-FDG and <sup>18</sup>F-FMISO PET/CT (DICOM), as well as BTV<sub>m</sub> (<sup>18</sup>F-FDG<sub>BTV</sub>) and BTV<sub>h</sub> (<sup>18</sup>F-FMISO<sub>BTV</sub>) (DICOM-RT), were transferred back to the local radiation oncologist by the same network.

In addition, the <sup>18</sup>F-FDG and <sup>18</sup>F-FMISO images on PET after the induction chemotherapy (PET<sub>1</sub>) and during radiotherapy (PET<sub>2</sub> at 40–46 Gy) were used to calculate the maximum SUVs (PET<sub>SUVmax1</sub> and PET<sub>SUVmax2</sub>)—that is, the highest-activity pixel value in the BTVs—and the percentages of variation in SUV<sub>max</sub> (Δ%<sub>SUVmax</sub>) and BTV (Δ%BTV). The SUV<sub>mean</sub> yielded results similar to those of the SUV<sub>max</sub> and are not presented here.

### Radiochemotherapy Protocol

The microscopic extension around the BTV<sub>m</sub> (clinical target volume [CTV]) was obtained either by isotropic expansion around the tumor (6 mm for squamous cell carcinoma, 8 mm for adenocarcinoma) (11) or by delineation of the <sup>18</sup>F-FDG PET/CT-positive mediastinal nodes (12). The isotropic CTV margin around the BTV<sub>h</sub> was set to 5 mm. The margin for the planning target volume (PTV) was 10 mm around the CTV (possibly 15 mm in the cranio-caudal direction) to take into account internal movements and uncertainties in positioning.

All the dose calculations were corrected for heterogeneity. Intensity-modulated radiotherapy (IMRT) was not allowed. The total dose was prescribed by the International Commission for Radiation Units point. The dose delivered in the PTV had to be within 95% and 107% of the prescribed dose. The target total dose was 86 Gy, provided that the maximum dose to the spinal cord was strictly less than 46 Gy and that no more than 30% of the total lung volume (excluding the gross tumor volume) received more than 20 Gy.

**TABLE 3**  
Acute Toxicity at 3 Months for 54 Included Patients

Acute adverse events	Hypoxia (n = 34), trial arm						No hypoxia		
	Boost (n = 24)			66 Gy (n = 10)			66 Gy (n = 20)		
	G1&2	G3	G4&5	G1&2	G3	G4&5	G1&2	G3	G4&5
Asthenia	5			6	1		1		
Pain	2			1			4		
Thoracic pain	5			2					
Dysphagia	17	1		6	3	1	11	4	
Dyspnea	1			3	1		6		
Hemoptysis	1					1 (G5)	1		
Dry skin or pruritus	15			1	1		9		
Anorexia	3			2			3		
Pneumonitis		2	1 (G4)				3		
Cough or expectoration	16			6			11		
Hematologic toxicities	2	1		1	1		4	2	1 (G4)
Chemotherapy toxicities	25	3		7	5		12	2	1 (G4)
Other toxicities	1						5		

As minor constraints, no more than 30% of the esophagus or the heart could receive more than 50 or 35 Gy, respectively.

The patients received 5 daily fractions of 2 Gy every week, with all the beams being treated daily. The shape of each beam was checked (electronic portal image) on the first fraction. The position of the isocenter was imaged daily (by orthogonal image or cone-beam CT scanner). Concomitant chemotherapy was *cis*-platinum (50 mg/m<sup>2</sup> days 1, 8, 29, and 36) and etoposide (50 mg/m<sup>2</sup> days 1–5, and 29–33) or *cis*-platinum (80 mg/m<sup>2</sup> days 1 and 22) and vinorelbine (15 mg/m<sup>2</sup> days 1, 8, 22, and 29). *Cis*-platinum could be replaced by carboplatin AUC 5 in the case of renal insufficiency.

#### Follow-up Procedures

The efficacy and toxicity assessments were planned at 3 mo and 1 y after the end of treatment (clinical examination, CT scanner).

#### Endpoints

The primary endpoint was the tumor response on CT scan at 3 mo (RECIST 1.1). Complete response (CR) was defined as no residual tumor image. Partial response (PR) was defined as a more than 30% reduction in maximal diameter. Progressive disease was defined as a more than 20% increase in the maximal diameter, whereas variations between –30% and +20% were classified as stable disease. The secondary endpoints were early and late toxicity (Common Terminology Criteria for Adverse Events) as well as DFS and OS at 1 y from definitive inclusion.

#### Sample Size

This open-label, single-arm, nonrandomized, multicenter phase II study followed a Gehan 2-step design. In the first step, 6 patients had to be evaluable 3 mo after completion of treatment. If no CR or PR

**TABLE 4**  
Late Toxicity for 54 Included Patients (1 Year)

Late adverse events	Hypoxia (n = 34), trial arm						No hypoxia		
	Boost (n = 24)			66 Gy (n = 10)			66 Gy (n = 20)		
	G1&2	G3	G4&5	G1&2	G3	G4&5	G1&2	G3	G4&5
Asthenia	2			1			2		
Pain	1			1	1				
Thoracic pain	1			1					
Dysphagia									
Dyspnea	5			3			4		
Dry skin or pruritus	1						1		
Pneumonitis							1		
Peripheral neuropathy							1		
Cough or expectoration	5			5			1		
Chemotherapy toxicities	3						1		
Others toxicities	2						1		

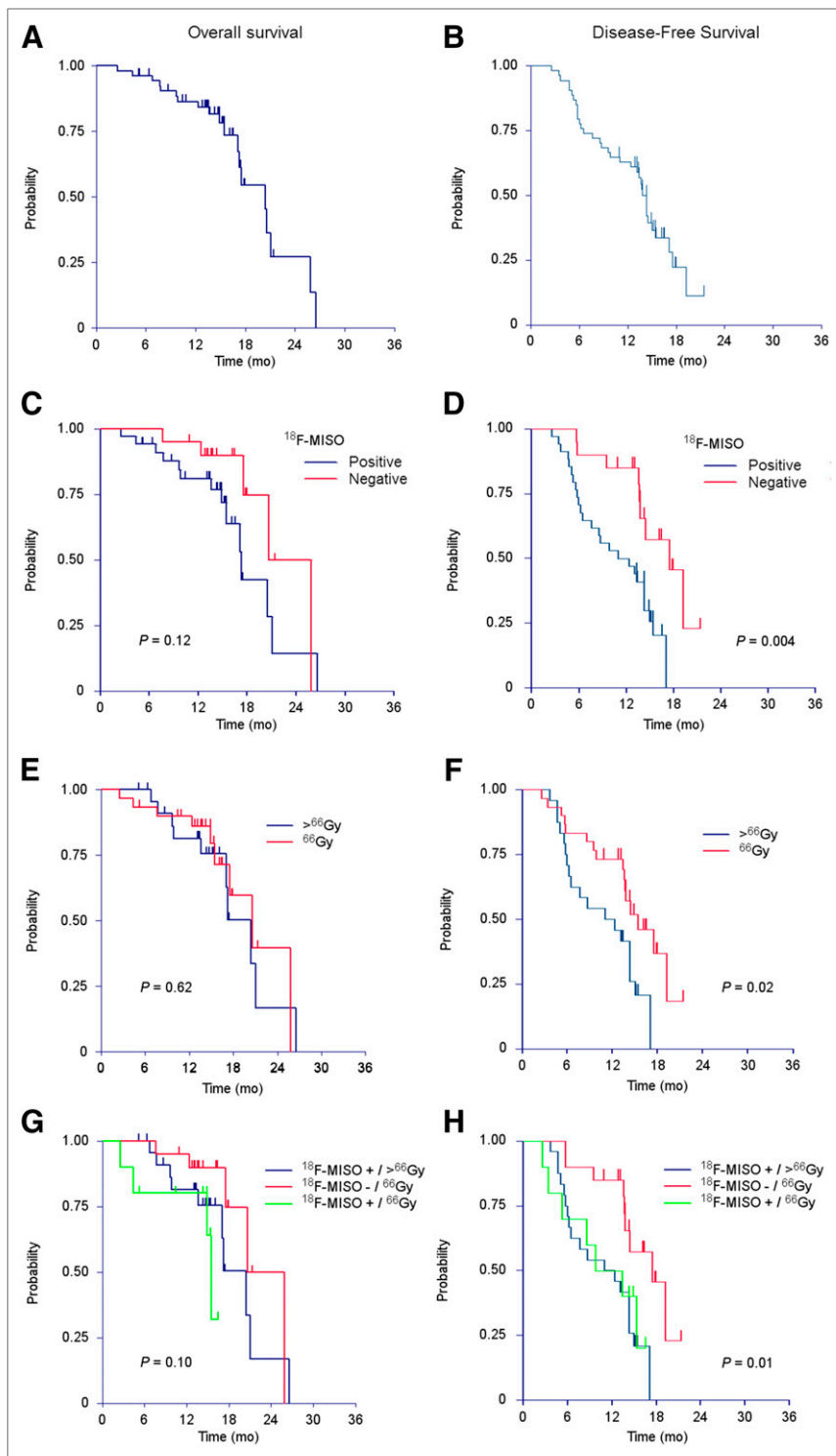


**FIGURE 2.** OS (left) and DFS (right), for entire population (A and B) as well as separation for the  $^{18}\text{F}$ -FMISO PET result (C and D), dose radiation (E and F), and both  $^{18}\text{F}$ -FMISO PET and dose radiation (G and H).

was observed, a response rate of more than 40% would be excluded, with 95% power and accrual stopped. If at least 1 response was observed, the number of additional patients to be entered in step 2 was calculated assuming an a priori response rate (complete or partial) of 40%, power  $1 - \beta = 95\%$ , precision  $\epsilon = 10\%$  and the number of responses in step 1, that is, 19, 18, 15, and 8 additional patients if 1, 2, 3, or 4 responses in step 1, respectively.

The number of patients to include was calculated as follows to obtain 25 patients evaluable at 3 mo (and 15 patients alive at 1 y, a 50% OS probability). Assuming 5 deaths/lost for follow-up at 3 mo, 30 patients with hypoxic lesions should be recruited and receive CCRT. Assuming that 50% of  $^{18}\text{F}$ -FMISO PET/CT would demonstrate the presence of hypoxic lesions, 60 preincluded patients should have persistent  $^{18}\text{F}$ -FDG uptake on the postinduction chemotherapy  $^{18}\text{F}$ -FDG PET/CT. We anticipated that 20% of the patients would have a negative  $^{18}\text{F}$ -FDG PET/CT result after induction chemotherapy (9). Therefore, a total of 75 patients would have to be preincluded. The 30 patients without  $^{18}\text{F}$ -FMISO-avid lesions would be monitored for 1 y (a secondary endpoint).

### Statistical Analysis

All analyses were conducted according to intent to treat, for example, irrespective of the radiotherapy total dose that was actually delivered. Descriptive statistics ( $n$ , mean, SD minimum and maximum) were calculated for the quantitative variables. Frequency and percentages with 95% confidence intervals (CIs) were determined for the qualitative variables. A Levene test was used to assess the equality of variances before comparing the quantitative variables between 2 or more groups (ANOVA). The survival probabilities were compared with a log-rank test. All the significance thresholds were set at 0.05 (2-tailed test). All the statistics were performed using SPSS software (version 20.0; IBM).

## RESULTS

### Patient Characteristics, Flowchart, and Descriptive Results

The study flow is shown in Figure 1. Seventy-nine patients were preincluded, and 54 patients were definitely included. The reasons for noninclusion were as follows: 8 inadequate procedures, 9 metastases and 3 with an absence of uptake on the  $^{18}\text{F}$ -FDG PET/CT, 4 consent withdrawals, and 1 investigator's decision. Thirty-four patients were eligible for the experimental group ( $^{18}\text{F}$ -FDG $_1$ -positive and  $^{18}\text{F}$ -FMISO $_1$ -positive).

The 54 definitively included patients were predominantly men (7 women and 47 men), with a mean age  $\pm$  SD of  $60.3 \pm 7.7$  y (Table 1). The histologic subtypes were 26 (48%) squamous cell carcinomas, 21 (39%) adenocarcinomas, and 7 (13%) undifferentiated carcinomas. The disease stages were mostly IIIA and IIIB. The descriptive data of the 79 preincluded patients were not significantly different (data not shown).

In the experimental arm, 24 of 34 (71%) patients received increased radiotherapy total doses (86 Gy, 5 patients; 80 Gy, 2; 76 Gy, 8; 74 Gy, 5, 72 Gy, 2). Because of organ-at-risk constraints, the dose was limited to 66 Gy in 10 patients. Among

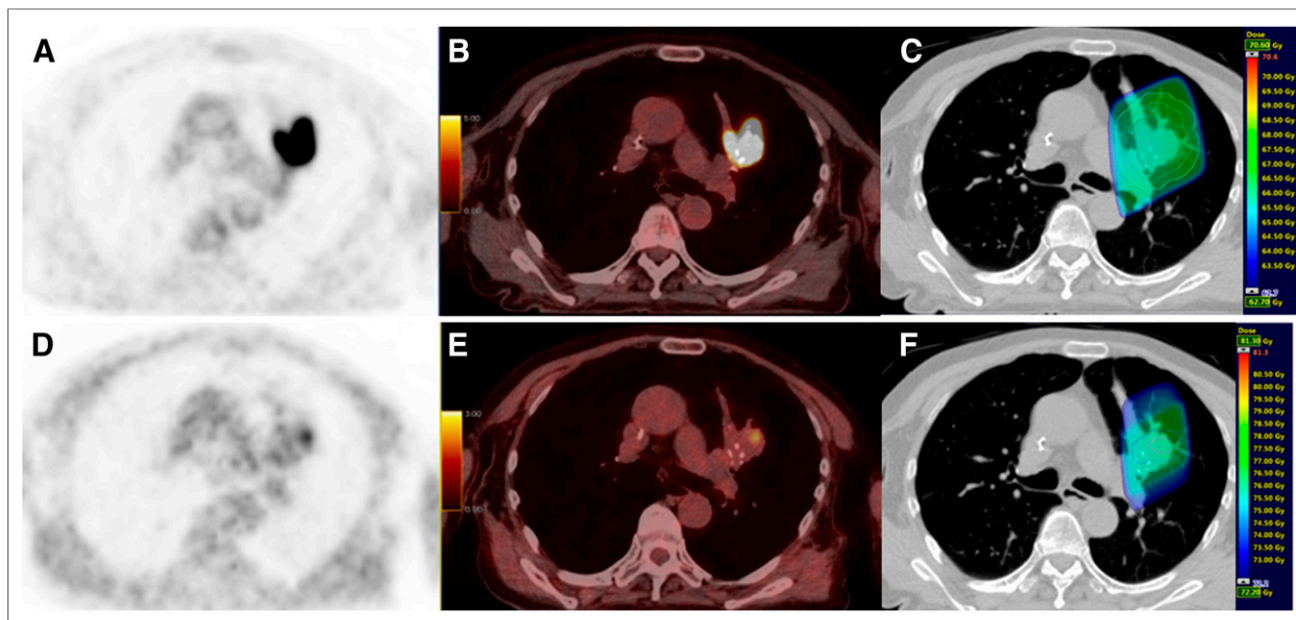


**FIGURE 3.** Example of patient with upper left lung NSCLC:  $^{18}\text{F}$ -FDG (A);  $^{18}\text{F}$ -FDG PET/CT (B); planning radiotherapy based on  $^{18}\text{F}$ -FDG (66 Gy) with  $\text{BTV}_m$  (gross tumor volume), CTV, and PTV (C); PET  $^{18}\text{F}$ -FMISO (D);  $^{18}\text{F}$ -FMISO PET/CT (E); and boost based on  $^{18}\text{F}$ -FMISO PET (76 Gy) with  $\text{BTV}_i$  and PTV boost (F).

the 20 patients without  $^{18}\text{F}$ -FMISO uptake, 19 received 66 Gy, and 1 received 68 Gy.

#### PET Description

The PET data are reported in Table 2. For the 54 included patients, the 54  $^{18}\text{F}$ -FDG<sub>1</sub> and 54  $^{18}\text{F}$ -FMISO<sub>1</sub> were available before the CCRT. In the 34 of 54 patients with hypoxia, 32 of 34  $^{18}\text{F}$ -FDG<sub>2</sub>, and 31 of 34  $^{18}\text{F}$ -FMISO<sub>2</sub> could be performed during the CCRT at 42 Gy (missing PETs because of medical or technical problems). The mean time intervals between injection and imaging were 66 (SD = 10) and 236 (SD = 6) min for the  $^{18}\text{F}$ -FDG and  $^{18}\text{F}$ -FMISO PET/CT, respectively. A total of 103 lesions (40 primary tumors and 63 nodes) were observed in the 54 patients. The per-patient and per-lesion analyses gave similar results. We present only per-patient PET data.

The patients with hypoxic lesions had significantly higher  $^{18}\text{F}$ -FMISO<sub>1</sub>  $\text{SUV}_{\text{max}}$  than the patients without hypoxia ( $P < 0.001$ ). Similarly, the patients with hypoxia had higher  $^{18}\text{F}$ -FDG  $\text{SUV}_{\text{max}1}$  ( $P = 0.02$ ) and larger  $^{18}\text{F}$ -FDG<sub>BTV1</sub> tumor volumes ( $P = 0.03$ ). The  $\text{BTV}$ s delineated on PET after the induction chemotherapy were approximately 40% smaller with  $^{18}\text{F}$ -FMISO than with  $^{18}\text{F}$ -FDG (SD = 54%), without statistically significant differences between the radiotherapy dose groups. For the 34 hypoxic patients who underwent  $^{18}\text{F}$ -FDG ( $n = 32$ ) and  $^{18}\text{F}$ -FMISO ( $n = 31$ ) during CCRT,  $^{18}\text{F}$ -FDG  $\text{SUV}_{\text{max}}$ ,  $^{18}\text{F}$ -FDG<sub>BTV</sub>, and  $^{18}\text{F}$ -FMISO  $\text{SUV}_{\text{max}}$  significantly decreased during CCRT.

#### Toxicity

Acute and late toxicities are listed in Tables 3 and 4, respectively. There was 1 grade 4 acute pneumonitis case among the 24 patients who received escalated radiotherapy doses. Three acute grade 4 toxicities were observed in the patients having received 66 Gy (whatever their  $^{18}\text{F}$ -FMISO uptake). One death (hemoptysis) occurred before the evaluation at 3 mo among the 10 patients with  $^{18}\text{F}$ -FMISO uptake and having received 66 Gy. No grade 4 or 5 late radiotherapy-related adverse events or acute/late cardiac toxicities were re-

ported in the entire population. The causes of the 19 reported deaths are described below.

#### Tumor Response and Survival

The survival curves are presented in Figure 2. The tumor response was evaluated at 3 mo ( $\pm 7$  d). The patient who died before evaluation at 3 mo in the  $^{18}\text{F}$ -FMISO-positive/66-Gy group was considered as having a nonresponding tumor. The response (CR+PR) rate at 3 mo was 31 of 54 (57% with 95% CI, 43%–71%). The corresponding figures were 17 of 34 (50%; 95% CI, 34%–66%) in the patients with  $^{18}\text{F}$ -FMISO uptake versus 14 of 20 (70%; 95% CI, 48%–85% in the patients without uptake ( $P = 0.25$ ). In the  $^{18}\text{F}$ -FMISO-positive patients, the response rates were 12 of 24 (50%; 95% CI, 31%–69%) after the escalated radiotherapy doses and 5 of 10 (50%; 95% CI, 24%–76%) after 66 Gy.

At the date of point, 35 patients were alive (a median follow-up duration of 14 mo [range 5–21 mo]), and 19 were alive without disease (15 mo [range, 11–21 mo]). Sixteen of the 19 deaths were due to cancer (9/10 in the high-radiotherapy-dose group, 3/4 in the  $^{18}\text{F}$ -FMISO-positive group, and 4/5 in the  $^{18}\text{F}$ -FMISO-negative group). The patient in the  $^{18}\text{F}$ -FMISO-positive/66-Gy group who died at 3 mo was discussed above. One patient in the high-radiotherapy-dose group was receiving nivolumab for progression under pemetrexed/bevacizumab maintenance. He died at home 17 mo after inclusion, and the cause of death remains unknown (drug toxicity or tumor progression). One patient in the  $^{18}\text{F}$ -FMISO group, without previous documentation of a relapse, was admitted to a palliative care unit with cognitive impairment, fever, and intestinal bleeding. He refused investigations and died at 18 mo. The OS and DFS probabilities at 1 y for the entire group were 0.86 (95% CI, 0.77–0.96) and 0.63 (95% CI, 0.49–0.74). Regarding the  $^{18}\text{F}$ -FMISO uptake, the OS at 1 y was 0.81 (95% CI, 0.67–0.95) when positive and 0.95 (95% CI, 0.85–1.0) when negative ( $P = 0.12$ ). The DFS at 1 y was 0.50 (95% CI, 0.32–0.65) and 0.85 (95% CI, 0.60–0.95), respectively ( $P = 0.004$ ). The DFS was lower after radiotherapy doses larger than 66 Gy (0.50 [95% CI, 0.29–0.68] vs. 0.73 [95% CI, 0.54–0.86],



$P = 0.02$ ). In the  $^{18}\text{F}$ -FMISO–positive patients, the DFS was similar regardless of whether the radiotherapy dose was 66 Gy (0.50 [95% CI, 0.18–0.75]) or higher (0.50 [95% CI, 0.29–0.68]).

## DISCUSSION

Our purpose was to increase the total dose of radiotherapy in the hypoxic parts of NSCLC in patients who were candidates for curative-intent chemoradiotherapy. Hypoxia has been shown to strongly reduce the radiosensitivity of tumor cells and to be associated with local failure (7). In this study, a key issue was to timely provide the radiation oncologists with a reliable target, anatomically and functionally defined, in a prospective multicenter setting. We have demonstrated that hypoxic areas were identified using  $^{18}\text{F}$ -FMISO PET in 34 of 54 patients (15 centers) and that higher radiotherapy doses (70–86 Gy) could be delivered without excessive toxicity in 24 patients with hypoxic areas. There were no statistically significant differences in the tumor response rates at 3 mo, and the OS at 1 y was similar among the 3 treatment groups. The DFS probability was significantly lower in the  $^{18}\text{F}$ -FMISO–positive patients, regardless of the radiotherapy dose. To our knowledge, we present the largest series of patients with NSCLC receiving radiotherapy boosted based on the hypoxia PET/CT in multicentric and prospective conditions.

As a targeted treatment, radiotherapy critically depends on accurate delineation of the volumes to be irradiated. A conventional CT scan is necessary for planning (Hounsfield units being correlated to electronic densities) and for drawing the anatomic contours of the tumor and the organs at risk. As for functional information (e.g., glucose metabolism with  $^{18}\text{F}$ -FDG), the PET/CT images must be either acquired in the treatment position or registered onto the planning CT.  $^{18}\text{F}$ -FMISO is one of several tracers that accumulate in hypoxic areas (13) and was selected for this study because it is commercially available. Although this study was ongoing, the MAASTRO group demonstrated (using HX4) that hypoxia images were stable when PET/CT was repeated (14) and provided a representation of the tumor functional status that was different from  $^{18}\text{F}$ -FDG images (15). A planning study of 10 patients by the same group showed that hypoxia images could be used to consider delivering heterogeneous doses to the tumor, specifically higher doses to hypoxic areas (16). All the PET tracers of hypoxia yield a relatively low signal-to-noise ratio. Therefore, the initial step of this study was to validate a reproducible method to identify the tumors with hypoxic areas and delineate BTVs for radiotherapy (8). The patients with hypoxia were identified by at least 3 trained experts, and the delineation of all the BTVs was centralized in 1 center. An example of  $^{18}\text{F}$ -FDG and  $^{18}\text{F}$ -FMISO images with BTV are presented in Figure 3.

We did not gate our PET acquisitions on breathing movements. Because  $^{18}\text{F}$ -FMISO uptake is known to be low in lung tumors ( $\text{SUV}_{\text{max}} = 2.5 [\pm 0.7]$  in our study), good-quality images cannot be obtained in respiratory gated mode, either for SUV measurement or for  $\text{BTV}_h$  delineation. Our criteria for  $\text{BTV}_h$  delineation was validated in free-breathing patients. We chose not to add further complexity to our design by requiring gated PET acquisitions and, for the sake of consistency, irradiations. In addition, mobile tumors are usually small and located in the parenchyma whereas most stage III tumors are large (and take up  $^{18}\text{F}$ -FMISO) and involve the mediastinum, that is, are mostly fixed. Lin et al. (17) have suggested a low reproducibility of  $^{18}\text{F}$ -FMISO PET images performed within 48 h. More recently, a preclinical study by Busk et al. (18) showed a good reproducibility of PET FAZA images

acquired within 48 h ( $r = 0.82$ ; range, 0.72–0.90), and Zegers et al. demonstrated the reproducibility of PET HX4 images in a human study (14). Mathematic simulations based on microscopic tumor tissue sections compared  $^{18}\text{F}$ -FMISO, FAZA, and HX4 and showed that  $^{18}\text{F}$ -FMISO provides a robust and reproducible signal 4 h after injection, with a lower contrast (19). Our observation that  $^{18}\text{F}$ -FMISO–avid tumors have a much worse prognosis confirms that hypoxia imaged on a single PET acquisition is a strong prognostic indicator, making it a relevant target volume for selective radiotherapy dose increase.

Radiobiologic and clinical data (7) suggest that total doses above 80 Gy are required to achieve tumor control in NSCLC. The RTOG 0617 (4) randomized trial reported reduced OS probabilities in patients receiving 74 Gy (vs. 60 Gy) in a target volume (median, 90 cc) defined on  $^{18}\text{F}$ -FDG PET/CT. Phase I–II studies have shown that doses in excess of 80 Gy could only be delivered to small tumors (2,3). Our BTVs delineated on  $^{18}\text{F}$ -FMISO PET/CT are approximately 40% smaller than those delineated on  $^{18}\text{F}$ -FDG PET/CT. Our results indicate that  $^{18}\text{F}$ -FMISO uptake is associated with a worse outcome, regardless of the radiotherapy total dose. An increased  $^{18}\text{F}$ -FMISO uptake was correlated with other poor prognosis features (larger tumor size, higher  $^{18}\text{F}$ -FDG  $\text{SUV}_{\text{max}}$ ), and hypoxia might not be the sole reason for treatment failure. The absence of  $^{18}\text{F}$ -FMISO uptake identifies a group of tumors with better prognosis. Our OS and DFS at 1 y compare favorably with those reported by RTOG 0617 (0.80 [95% CI, 0.74–0.85] and 0.49 [95% CI, 0.42–0.56], respectively) in their patients treated to 60 Gy (4). Similar approaches are being evaluated in clinical trials increasing total dose to smaller subvolumes that are considered at higher risk of failure (high  $^{18}\text{F}$ -FDG uptake subvolumes on preradiotherapy  $^{18}\text{F}$ -FDG PET/CT (RTOG 1106 NCT01507428, PET Boost NCT01024829), residual tumor at mid-treatment  $^{18}\text{F}$ -FDG PET/CT (RTEP 7, NCT02473133)).

An extensive discussion about radiotherapy dose and delivery is beyond the scope of the present paper. Briefly, our patients were irradiated with a 3-dimensional conformal technique. When our trial was designed, IMRT was available in too few French centers. IMRT was used in approximately 50% of the RTOG 0617 patients with outcomes similar to 3-dimensional RT (4). The dosimetry benefits of IMRT have not been confirmed in a randomized trial (20). The dosimetry of protons is characterized by localized high-dose delivery and sharp fall-out (Bragg peak) (21). No significant differences in tumor outcome were observed in a randomized comparison of 3-dimensional proton therapy versus IMRT (22). Radiotherapy in stereotactic conditions is an accepted treatment for tumors up to 65 cc, provided that strict organ at risk dose–volume constraints are met (23). Our patients had mean  $^{18}\text{F}$ -FMISO–avid volumes of 33.5 cc, with large variability (SD = 52.2 cc; range, 1–234 cc). A few additional fractions could be delivered, intended as a concomitant boost, whereas the  $^{18}\text{F}$ -FDG–defined target volume is treated conventionally (2 Gy per fraction), keeping the treatment duration around 6–7 wk. The positive results of accelerated radiotherapy (24) suggest that tumor proliferation during radiotherapy might have contributed to the failure of escalated radiotherapy dosage delivered over a protracted treatment time to improve the outcome in NSCLC (4).

## CONCLUSION

This prospective phase II study demonstrates the feasibility of delivering higher radiotherapy doses to smaller target volumes identified by  $^{18}\text{F}$ -FMISO uptake without exceeding the tolerance



to the normal organs. The benefit of this approach, possibly with larger doses per fraction in stereotactic conditions as a concomitant boost, remains to be investigated in a randomized trial.

## DISCLOSURE

This study was supported by a grant from the French National Cancer Institute (PHRC 2011). No other potential conflict of interest relevant to this article was reported.

## ACKNOWLEDGMENTS

We thank the patients who agreed to participate in this study and their respective referring pneumologists, nuclear medicine physicians, and radiation oncologists from the participating centers. We also thank the technologists from the Department of Nuclear Medicine (Centre Henri Becquerel) for their help in managing the patients. We are particularly thankful to Olivier Rastelli, Lucie Burel, Pierrick Gouel, Céline Breton, Dorianne Richard, and Dr. Louis-Ferdinand Pepin for their excellent collaboration.

## REFERENCES

1. Ball D. Curing non-small cell lung cancer with radiotherapy: no longer an oxymoron. *Semin Radiat Oncol.* 2015;25:65–66.
2. Kong FM, Ten Haken RK, Schipper MJ, et al. High-dose radiation improved local tumor control and overall survival in patients with inoperable/unresectable non-small-cell lung cancer: long-term results of a radiation dose escalation study. *Int J Radiat Oncol Biol Phys.* 2005;63:324–333.
3. van Baardwijk A, Wanders S, Boersma L, et al. Mature results of an individualized radiation dose prescription study based on normal tissue constraints in stages I to III non-small-cell lung cancer. *J Clin Oncol.* 2010;28:1380–1386.
4. Bradley JD, Paulus R, Komaki R, et al. Standard-dose versus high-dose conformal radiotherapy with concurrent and consolidation carboplatin plus paclitaxel with or without cetuximab for patients with stage IIIA or IIIB non-small-cell lung cancer (RTOG 0617): a randomised, two-by-two factorial phase 3 study. *Lancet Oncol.* 2015;16:187–199.
5. Aerts HJ, Bussink J, Oyen WJ, et al. Identification of residual metabolic-active areas within NSCLC tumours using a pre-radiotherapy FDG-PET-CT scan: a prospective validation. *Lung Cancer.* 2012;75:73–76.
6. Calais J, Thureau S, Dubray B, et al. Areas of high <sup>18</sup>F-FDG uptake on preradiotherapy PET/CT identify preferential sites of local relapse after chemoradiotherapy for non-small cell lung cancer. *J Nucl Med.* 2015;56:196–203.
7. Horsman MR, Wouters BG, Joiner MC, Overgaard J. The oxygen effect and fractionated radiotherapy. In: Joiner MC, van der Kogel A, eds. *Basic Clinical Radiobiology*. 4th. ed. Boca Raton, FL: Talyor & Francis Group, NW; 2009.
8. Thureau S, Chaumet-Riffaud P, Modzelewski R, et al. Interobserver agreement of qualitative analysis and tumor delineation of <sup>18</sup>F-fluoromisonidazole and 3'-deoxy-3'-<sup>18</sup>F-fluorothymidine PET images in lung cancer. *J Nucl Med.* 2013;54:1543–1550.
9. Edet-Sanson A, Dubray B, Doyeux K, et al. Serial assessment of FDG-PET FDG uptake and functional volume during radiotherapy (RT) in patients with non-small cell lung cancer (NSCLC). *Radiother Oncol.* 2012;102:251–257.
10. Boellaard R, Delgado-Bolton R, Oyen WJG, et al. FDG PET/CT: EANM procedure guidelines for tumour imaging: version 2.0. *Eur J Nucl Med Mol Imaging.* 2015;42:328–354.
11. Giraud P, Antoine M, Larrouy A, et al. Evaluation of microscopic tumor extension in non-small-cell lung cancer for three-dimensional conformal radiotherapy planning. *Int J Radiat Oncol Biol Phys.* 2000;48:1015–1024.
12. Chapet O, Kong FM, Quint LE, et al. CT-based definition of thoracic lymph node stations: an atlas from the University of Michigan. *Int J Radiat Oncol Biol Phys.* 2005;63:170–178.
13. Lopci E, Grassi I, Chiti A, et al. PET radiopharmaceuticals for imaging of tumor hypoxia: a review of the evidence. *Am J Nucl Med Mol Imaging.* 2014;4:365–384.
14. Zegers CM, van Elmpt W, Szardenings K, et al. Repeatability of hypoxia PET imaging using [<sup>18</sup>F]HX4 in lung and head and neck cancer patients: a prospective multicenter trial. *Eur J Nucl Med Mol Imaging.* 2015;42:1840–1849.
15. Zegers CM, van Elmpt W, Reymen B, et al. In vivo quantification of hypoxic and metabolic status of NSCLC tumors using [<sup>18</sup>F]HX4 and [<sup>18</sup>F]FDG-PET/CT imaging. *Clin Cancer Res.* 2014;20:6389–6397.
16. Even AJ, van der Stoep J, Zegers CM, et al. PET-based dose painting in non-small cell lung cancer: comparing uniform dose escalation with boosting hypoxic and metabolically active sub-volumes. *Radiother Oncol.* 2015;116:281–286.
17. Lin Z, Mechalakos J, Nehmeh S, et al. The influence of changes in tumor hypoxia on dose-painting treatment plans based on <sup>18</sup>F-FMISO positron emission tomography. *Int J Radiat Oncol Biol Phys.* 2008;70:1219–1228.
18. Busk M, Mortensen LS, Nordmark M, et al. PET hypoxia imaging with FAZA: reproducibility at baseline and during fractionated radiotherapy in tumour-bearing mice. *Eur J Nucl Med Mol Imaging.* 2013;40:186–197.
19. Wack LJ, Mönlich D, van Elmpt W, et al. Comparison of [<sup>18</sup>F]-FMISO, [<sup>18</sup>F]-FAZA and [<sup>18</sup>F]-HX4 for PET imaging of hypoxia: a simulation study. *Acta Oncol.* 2015;54:1370–1377.
20. Price A. Intensity-modulated radiotherapy, not 3 dimensional conformal, is the preferred technique for treating locally advanced disease with high-dose radiotherapy: the argument against. *Semin Radiat Oncol.* 2015;25:117–121.
21. Chang JY, Jabbour SK, De Ruyscher D, et al. International Particle Therapy Cooperative Group Thoracic Subcommittee: consensus statement on proton therapy in early-stage and locally advanced non-small cell lung cancer. *Int J Radiat Oncol Biol Phys.* 2016;95:505–516.
22. Liao ZX, Lee JJ, Komaki R, et al. Bayesian randomized trial comparing intensity modulated radiation therapy versus passively scattered proton therapy for locally advanced non-small cell lung cancer [abstract]. *J Clin Oncol.* 2016;34(15, suppl):8500.
23. Shultz DB, Diehn M, Loo BW Jr. To SABR or not to SABR? Indications and contraindications for stereotactic ablative radiotherapy in the treatment of early-stage, oligometastatic, or oligoprogressive non-small cell lung cancer. *Semin Radiat Oncol.* 2015;25:78–86.
24. Saunders M, Dische S, Barrett A, Harvey A, Griffiths G, Palmar M. Continuous, hyperfractionated, accelerated radiotherapy (CHART) versus conventional radiotherapy in non-small cell lung cancer: mature data from the randomized multicentre trial. CHART Steering committee. *Radiother Oncol.* 1999;52:137–148.